Bull. Chem. Soc. Jpn., 72, 151—162 (1999)

Headline Articles

Density Fluctuation and Hydrogen-Bonded Clusters in Supercritical Water. A Molecular Dynamics Analysis Using a Polarizable Potential Model

Noriyuki Yoshii, Shinichi Miura, and Susumu Okazaki*

Department of Electronic Chemistry, Tokyo Institute of Technology, 4259 Nagatsuta, Midori-ku, Yokohama 226-8502

(Received September 4, 1998)

A series of molecular dynamics calculations of supercritical (SC) water along an isotherm at 600 K have been performed using a polarizable potential model. A relatively large system composed of 1000 molecules was adopted to reproduce long-ranged density fluctuations in SC water. The oxygen–oxygen partial static structure factor has been calculated for various densities. The strong intensity of the static structure factor in the small wave number region has successfully been reproduced for the fluid near the critical point. The density fluctuation was investigated using a concept of "cluster," which was defined by a set of molecules connected by "bonds." In this paper, two kinds of bonds were adopted. One is a bond defined simply using the oxygen–oxygen distance (D-bond) and the other is a hydrogen bond (H-bond). Size distribution of both the D- and H-bond clusters was described well by Fisher's droplet model. These clusters have bulky structures compared with closely packed low temperature clusters, and can be regarded as "fractal." The larger the D- and H-bond clusters, the longer the relaxation times. Together with the size distribution of the clusters, this may give a molecular picture of critical slowing down.

In recent years, supercritical (SC) water has received remarkable attention in the field of industrial applications.[1—8] Various properties of SC water change dramatically with decreasing pressure and/or increasing temperature.[9,10] In particular, along an isotherm at SC temperature, density of the system is easily controlled by pressure since SC water has a large compressibility. This is common to the other SC fluids. The change of the density leads to a considerable change of the fluid properties, e.g. the dielectric constant. It is widely known that water at ambient condition has a large dielectric constant in comparison with other polar liquids. This comes from hydrogen bonds among water molecules, which forms a three-dimensional network of bonds.[11] As density decreases along the isotherm at SC temperature, the dielectric constant is substantially reduced due to a decrease of the number of the hydrogen bonds. The property allows us to change the solubility of ionic species as well as oily ones in water simply by controlling the pressure.[12] Thus, properties of supercritical fluids such as the above enable us to construct effective industrial process using a single solvent.

From a microscopic viewpoint, the large compressibility of the SC fluids is ascribed to the large density fluctuations of the fluid, which are represented by long-ranged pair correlations of particles. A possible microscopic analysis of the fluctuation may be given based on a concept of "cluster." We have shown that the picture works well, at least, for the simple SC fluids.[13] With respect to SC water, however, the hydrogen bond gives an additional complexity to the fluid properties, and little has been clarified for this. The purpose of the present paper is, thus, to throw light on the density fluctuations of SC water on a molecular level.

Long ranged density–density correlation is a key function to describe the properties of the SC fluids. This may be represented by the strong intensity of the static structure factor in small wave number (k) region, which has been investigated experimentally for various SC fluids.[14—16] From the behavior of the static structure factor at small k, the correlation length of the density fluctuation has been evaluated; the quantity represents a certain spatial size of the fluctuation. For SC water, however, neutron scattering experiments so far have mainly focused on short-ranged structure of the fluid.[17] Since interest has been concentrated upon persistence of the hydrogen bonds in SC water,[18,19] little has been discussed concerning the properties of the long-ranged density–density correlation. To our knowledge, few experimental studies of the molecular picture of the fluid structure and dynamics of this large density fluctuation have been reported.

The long ranged density fluctuation has been analyzed theoretically based on Fisher's droplet model.[20—22] Originally, this model was developed in order to obtain a physical

interpretation for the scaling relation found in the critical phenomena of gas–liquid and magnetic phase transitions. The model introduced a picture of the fluid near the critical point: the system consists of "droplets" or "physical cluster" of various sizes which do not interact with each other. The partition function for the fluid can, then, be explicitly calculated. However, it contains two phenomenological parameters, the so-called semi-phenomenological model. Further, as a generalization of this model, Stauffer introduced a scaling function in the percolation theory.[23] In this theory, the percolation threshold corresponds to the critical temperature for the liquid–gas phase transition. Thus, the theory is valid only for the fluid above and below the density near the percolation threshold. On the other hand, molecular dynamics (MD) calculation has been providing an actual atomistic picture for the theoretical model. In particular, with the help of percolation theory,[23] the MD calculation has demonstrated that the fluid can be described by an ensemble of clusters of various sizes below the percolation density using properly defined intermolecular bonds.[13] Each cluster corresponds to a droplet in the theoretical model. The calculation study of the SC Lennard–Jones (LJ) fluids has revealed that the cluster size distribution is well described by the droplet model.[13] The study also showed that the cluster has a "fractal" character,[13,24] showing that the high temperature clusters have bulky structures. The cluster in the SC fluids has successfully presented a molecular picture of the critical slowing down experimentally observed in the dynamic structure factor.[25–27] In the fluid near the critical point, large clusters appear in the system, which gives a slow relaxation in the above correlation function.

In this study, SC water has been investigated based upon MD calculation. In order to analyze the density fluctuation, a relatively large system composed of 1000 molecules was adopted, for which the static structure factor in small k region was calculated. The density fluctuation has been analyzed based on Fisher's droplet model. Here, two different intermolecular bonds were investigated. One is bond similar to that used previously for the LJ fluids,[13] and the other is the hydrogen bond which is specific to water. Analyses have been carried out separately for the clusters defined by the above two bonds.

The paper is organized as follows. Computational details are described in Sect. 1. Structural and dynamical properties of the clusters are presented in Sects. 2 and 3, respectively. We conclude in Sect. 4.

1. Computational Details

Molecular Dynamics Calculations. In this study, MD calculations of SC water have been performed for a wide range of density from gaslike one to liquidlike one. A polarizable potential model of water proposed by Dang (called RPOL model) was employed to take account of state-point dependence of intermolecular interaction.[28] The model consists of three interaction sites, corresponding to an oxygen atom and two hydrogen atoms. Each site has a fixed partial charge and isotropic atomic polarizability to describe long-ranged Coulomb interaction. Short-ranged repulsive interaction as well as weak dispersion interaction was presented by the LJ potential function as a function of oxygen–oxygen separation. Details of the calculation method were described elsewhere.[29] Critical constants for the RPOL model were reported previously to be $\rho_c = 0.30\ \mathrm{g\,cm^{-3}}$ and $T_c = 561$ K where ρ_c and T_c are the critical density and temperature, respectively.[30]

We performed the calculation for a relatively large system composed of 1000 molecules, since our primary interest is in the long-ranged density fluctuation. In order to test the system size, we composed the side length of cubic MD box L with the correlation length of static density correlation at $\rho = \rho_c$ and $T = 1.07\,T_c$. The system at this state point must have the longest correlation length among the states examined in this paper. The correlation length ξ can be estimated based on the equation for ξ proposed experimentally by Sengers et al.[9] The evaluated ξ is 11.2 Å at ρ_c and $1.07\,T_c$. The side length of the MD box at the same reduced condition was 46.7 Å, which is more than four times longer than the experimental ξ. Thus, we believe that our simulated system is large enough to describe the long-ranged density–density correlation in SC water.

The calculations were performed for seven selected state points along an isotherm at $1.07\,T_c$ (= 600 K). Density of the system ranges from liquidlike one to gaslike one: 1.00, 0.647, 0.441, 0.294, 0.147, 0.0735, and 0.0367 $\mathrm{g\,cm^{-3}}$, corresponding to $3.4\rho_c$, $2.2\rho_c$, $1.5\rho_c$, ρ_c, $\rho_c/2$, $\rho_c/4$, and $\rho_c/8$, respectively. For comparison, calculation of water at ambient condition ($1.00\ \mathrm{g\,cm^{-3}}$ and 300 K) was also performed. After an equilibration period of 15 ps, the calculation of the system was extended to 30 ps for the system at $1.00\ \mathrm{g\,cm^{-3}}$ and 300 K and at $3.4\rho_c$ and $1.07\,T_c$. The production runs for the system at lower densities were continued to 60 ps in order to obtain satisfactory statistics to calculate static structure factors at small wave number regions.

Definitions of Intermolecular Bond. In this paper, the density fluctuation is analyzed using the concept of "cluster." The cluster was defined by a set of molecules connected with each other by intermolecular "bonds." Two kinds of bonds were adopted. One is defined simply by oxygen–oxygen distance and the other is a hydrogen bond. The former is almost the same as the bond employed in the previous analysis for the clusters in the SC LJ fluid.[13] For a given pair of molecules, two molecules are regarded as bonded if the oxygen–oxygen distance is less than a threshold value. The threshold distance was chosen to be 1.24σ (= 3.96 Å) where σ is a diameter parameter of LJ potential for the oxygen atom. The distance corresponds to the inflection point of the LJ potential function. Hereafter, this bond is referred to as D-bond. On the other hand, the hydrogen (H-)bond was defined in the same manner as that used in our previous study.[29] According to this, the two molecules are regarded as hydrogen-bonded when both geometrical and energetical conditions are satisfied simultaneously;[31] the distance between oxygen and hydrogen atoms is shorter than threshold distance, 2.5 Å, and the interaction energy between

two molecules is lower than -14 kJ mol^{-1}. As shown in our previously paper, such a definition gives a reasonable number of hydrogen bonds per molecule for both the ambient and SC water.

2. Structure

Density-dependent static properties of SC water in seven physical states along an isotherm at 1.07 T_c have been examined. In particular, the long-ranged density fluctuation has been investigated calculating static structure factor. "Clusters" generated in SC water have also been analyzed in detail in order to obtain a microscopic picture of the density fluctuation.

Static Structure Factor. Calculated oxygen–oxygen partial static structure factors $S_{OO}(k)$ for seven state points along the isotherm at 1.07 T_c are shown in Fig. 1. For comparison, $S_{OO}(k)$ at 300 K and 1 g cm^{-3} is also presented. Wave numbers examined are in the range of $0.067 \leqq k \leqq 10$ Å^{-1}. The minimum wave number is determined from $k_{min} = 2\pi/L$, where L is the side length of the cubic MD box. In general, correlation of the long wavelength fluctuation converges to the average value very slowly. Thus, to test the statistics, we plotted the cumulative average of $S_{OO}(k)$ for the fluid at ρ_c in the figure, too, for three small wave numbers. The figure clearly shows that all the values satisfactorily converged to their averages within 20 ps. In order to estimate a statistical error of the calculation, we divided the trajectory of 60 ps into three blocks for the fluids at $\rho \leqq 2.2\rho_c$. Each block has a duration time of 20 ps. Then, an error bar was obtained representing the maximum and minimum values of the average for three 20 ps trajectories. For the fluids at $3.4\rho_c$ and 1.07 T_c and at 1.0 g cm^{-3} and 300 K, the 30 ps trajectories were divided into three to estimate the error bar since the cumulative averages converged well within 10 ps.

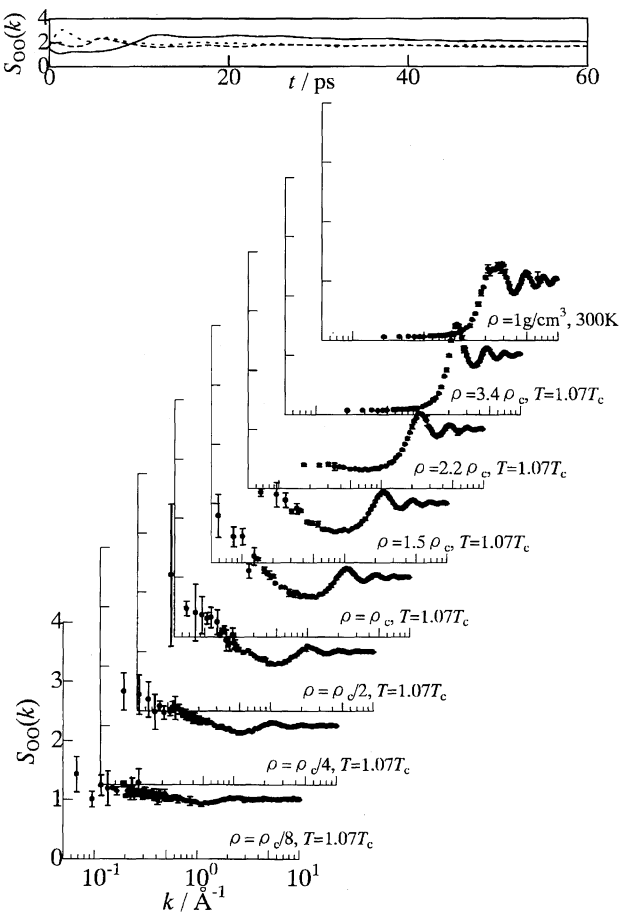

Fig. 1. Oxygen–oxygen static structure factor $S_{OO}(k)$ for SC water at various densities along the isotherm at T = 1.07 T_c. Error bars in the figure represent minimum and maximum values of $S_{OO}(k)$ among three averaged values of each 20 (or 10) ps trajectory obtained by dividing the total 60 (or 30) ps trajectory into three periods.

In the small wave number region ($k \leqq 0.5$ Å^{-1}), the intensity of $S_{OO}(k)$ becomes strong as the system approaches the critical density. The growing intensity observed in the small k region represents the long-ranged density-density correlation that is characteristic of the fluid near the critical point. The large density fluctuation in SC water was, thus, qualitatively reproduced by our calculations. To our knowledge, this is the first MD result for small-angle scattering of SC water. Now, in principle, we can estimate experimental quantities such as correlation length and isothermal compressibility from an Ornstein–Zernike–Debye plot for small k correlation.[16] However, as shown in the figure, the error in the calculated $S_{OO}(k)$ in the small k region is quite large. So we do not present such quantities here. Much larger-scale and longer-time MD calculations may be needed to discuss these kinds of parameters quantitatively.

D-Bond Clusters. Here, we analyze the density fluctuations shown in the previous subsection in terms of a cluster. In this subsection, analyses have been done for the D-bond clusters defined above. Analyses for the hydrogen-bonded clusters will be presented in the next subsection. Percolation of the D-bonds in the fluid is discussed, too. The definition of the percolation is the same as that employed in the previous study for the SC LJ fluids.[13] According to this, at $\rho \geqq \rho_c$, SC water was found to be above the percolation threshold. This means that the system can be regarded as a mixture of a percolated infinitely large cluster and small clusters. At $0.5\rho_c$, the fluid was below the percolation threshold. Then, the fluid may be regarded as an ensemble of clusters of various sizes. This indicates that the density where percolation occurs is between ρ_c and $0.5\rho_c$. For the LJ fluids, the percolation density ρ_p was $0.94\rho_c$, which is slightly smaller than the critical density. This is consistent with the present result for SC water. Since the purpose of the present work is to clarify a molecular picture of the density fluctuation, the precise value of ρ_p, which depends upon the definition of the bond, was not determined. The analyses of the clusters have been carried out for the fluids below the percolation density, i.e. $\rho \leqq 0.5\rho_c$.

In Fig. 2, the size distribution $f(s)$ of the clusters in the fluid at $\rho \leqq 0.5\rho_c$ is presented. Here, the size of cluster was defined as the total number of molecules which constitutes the cluster. The ordinate of the figure is $\ln(s^{2.1}f(s))$. It is interesting to find that each plot clearly shows a straight line.

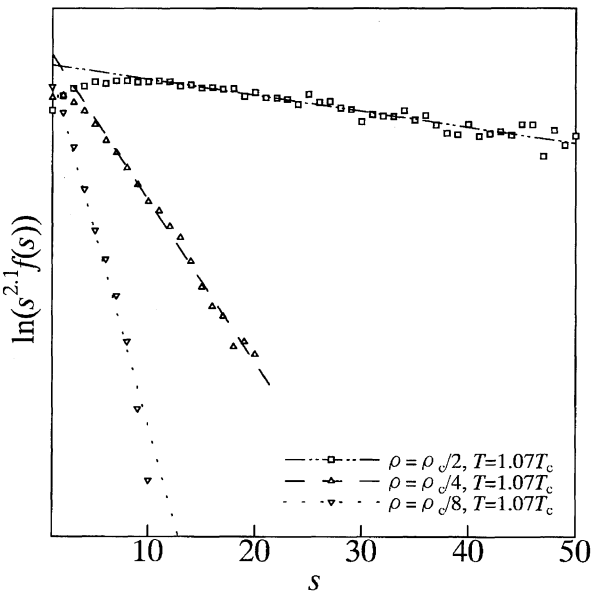

Fig. 2. Probability $f(s)$ that D-bond cluster is composed of s molecules for SC water at various densities along the isotherm at T = 1.07 T_c. In the figure, $\log s^{\tau} f(s)$ is plotted against s where the values σ = 0.5 and τ = 2.1 are adopted.

This indicates that the size distribution can be described by Fisher's droplet model;[20—22] the distribution $f(s)$ is of the form:

$$f(s) \propto s^{-\tau} \exp(-as^{2\sigma}), \quad (1)$$

where σ and τ are phenomenological parameters. The parameter σ is an exponent representing the variation of mean cluster surface area A_s as a function of cluster size s, $A_s \propto s^{\sigma}$. The parameter τ is called Fisher exponent, which has its origin in the entropy of the cluster.[22] Here, the parameters σ and τ were 0.5 and 2.1, respectively, which are the same as those adopted for the SC LJ fluid. Thus, the droplet model gives a good approximation to describe the D-bond clusters in SC water for all the densities below ρ_c. The slope of the plot represents parameter a in the model. This parameter must be a function of $\rho_p - \rho$, where ρ_p is the percolation density. At the percolation density, the parameter a must be zero. In fact, the figure shows that the slope becomes small as the density approaches ρ_p from the low density side. It is known that the cluster size distribution obtained from the adiabatic expansion of liquids at low temperature may be given by $f(s) \propto \exp(-as^{2\sigma})$.[32] This distribution corresponds to that of Fisher's droplet model with $\tau = 0$. Thus, at high temperature, the structure of the cluster is "entropically favorable" in contrast to those of the clusters generated at low temperature by adiabatic expansion processes. The entropically favorable structures of clusters are analyzed below in detail.

In Table 1, the averaged probabilities that particular topologies are found for the D-bonds in the cluster whose size is 3 and 4 are summarized for the fluid at various densities. It is clearly found that the clusters have relatively loosely packed structures. For example, the topology of the cluster with s = 3 is dominated by open structure; 85% of

Table 1. Averaged Probability That Particular Topologies Are Found for the D-Bonds in the Clusters Whose Size is 3 and 4 for the Fluid at Various Densities

s=3	$\rho_c/2$	$\rho_c/4$	$\rho_c/8$
	0.15	0.14	0.15
	0.85	0.86	0.85
s=4	$\rho_c/2$	$\rho_c/4$	$\rho_c/8$
	0.00	0.00	0.00
	0.05	0.04	0.04
	0.24	0.23	0.24
	0.02	0.01	0.01
	0.55	0.59	0.59
	0.14	0.13	0.12

the clusters have a chain structure, whereas closely packed triangle structure is only 15%. The clusters with s = 4 show a similar tendency, where the fraction of loop structures, is only 32%. The most densely packed tetrahedral structure was not found at all. The remaining clusters, 68%, have bulky structures. Further, it is interesting to find that the average probability of each topology is almost independent of the fluid density. This implies that the structure of the clusters in SC water along the isotherm is independent of density. This behavior was also observed for the clusters in the SC LJ fluid.[13]

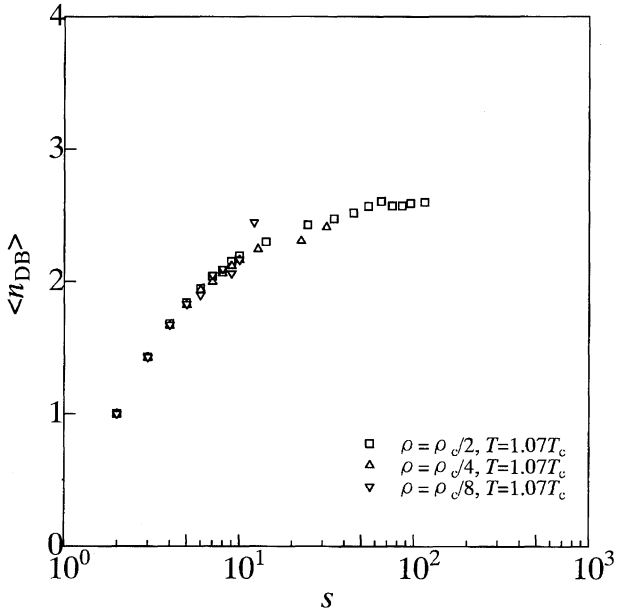

Fig. 3. Average number of D-bonds per molecule $\langle n_{DB} \rangle$ as a function of cluster size s for SC water at various densities along the isotherm at T = 1.07 T_c.

Averaged bond number $\langle n_{DB} \rangle$ is presented in Fig. 3 as a function of cluster size s. The number increases with increasing cluster size. For small clusters ($s \leqq 10$), $\langle n_{DB} \rangle$ grows up rapidly as s increases. For larger clusters ($s > 10$), however, $\langle n_{DB} \rangle$ increases slowly and seems to converge to a certain value. The former behavior may be ascribed to the decreasing ratio of the number of molecules at the cluster surface to that inside the cluster. The surface molecules must have a small number of bonds compared with the core molecules. This is clearly found in Fig. 4, where distribution of the number of the D-bonds per molecule is presented for a few ranges of cluster size. In the histogram, $n_{DB} = 1$ represents the molecules at the end of the bond network; $n_{DB} = 2$ is from the molecules constituting a straight chain. These must be found on the surface of the clusters. On the other hand, the molecules with $n_{DB} \geqq 3$ take part in branched network and must be located in relatively densely packed region in the clusters. This figure shows that a small cluster, $s = 9$, has a large number of molecules with $n_{DB} = 1$ and 2, whereas large clusters, $s = 41$—50, have a large distribution at $n_{DB} \geqq 3$. For the small cluster, most molecules must be the surface molecules. This results in a large distribution at $n_{DB} = 1$ and 2. On the other hand, the large clusters must have a number of molecules inside it, leading to the shift of the distribution to greater n_{DB}. Further, it is interesting to find that the distribution is almost the same between the clusters with $s = 41$—50 and $s = 91$—100. These clusters are large enough to show little surface effect, which also causes the saturation of $\langle n_{DB} \rangle$ found for large clusters in Fig. 3. For the fluid at all the densities examined here, the molecules have a relatively small number of bonds compared with the ones in the dense liquids, typically $n_{DB} = 12$;[33] the molecules which have a very small number of bonds ($n_{DB} \leqq 3$) occupy more than 70% of the molecules. Thus, even in the large clusters, there are few densely packed regions like liquids. This clearly shows that the clusters have a number of voids of various sizes inside them and most water molecules are on the perimeter. It should be noted, here, that from either Fig. 3, or Fig. 4, little density dependence is found. This is in correspondence to the finding that the topology of bond pattern is almost independent of the fluid density. The structure of the clusters is, thus, a bulky one in comparison with that found for the energetically stable clusters at low temperatures and has little density dependence.

In order to characterize the structure of the clusters in more detail, radius of gyration of the cluster is presented in Fig. 5 as a function of cluster size.[34] The value of s may be scaled according to $s \propto R_g^D$ where R_g is the radius of gyration of the cluster[13,35] and D is an exponent related to its spatial dimension. For closely packed cluster, D must be 3. For the present loosely packed clusters stated above, D should be less than 3. In this case, the cluster may be regarded as "fractal."[23] The fractal dimension D for the present high temperature cluster was evaluated to be about 2.2 from the log–log plot presented in Fig. 5. The value is very similar to that obtained for the LJ fluid, 2.25[13] The plots for the fluid at various densities present a single straight line, indicating again that the fractal dimension has little density dependence.

Hydrogen-Bonded Cluster. In this subsection, hydrogen-bonded cluster in SC water are analyzed. The cluster was defined as a set of water molecules connected by the hydrogen bonds. Prior to the detailed analysis, the hydrogen bonds were found to be percolated in the fluids at the density

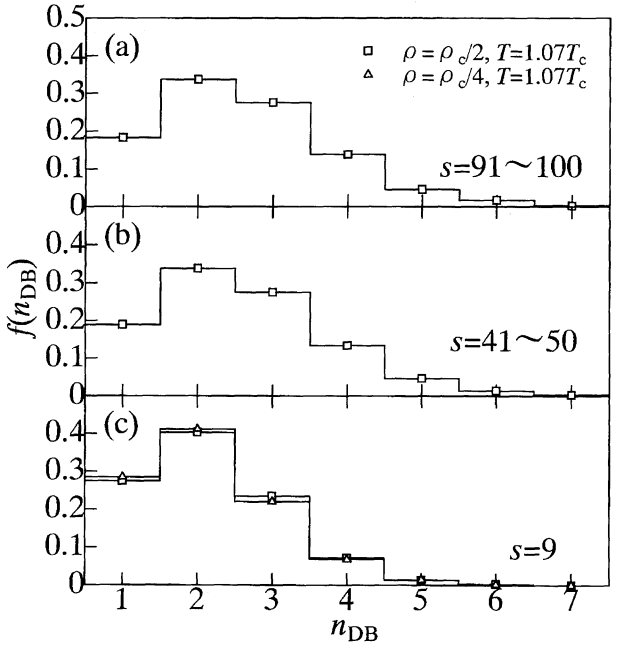

Fig. 4. Probability distribution of the number of D-bond per molecule n_{DB} for SC water at two densities, $\rho = \rho_c/2$ and $\rho_c/4$, for three classes of cluster size. (a) $s = 9$, (b) $41 \leqq s \leqq 50$, and (c) $91 \leqq s \leqq 100$.

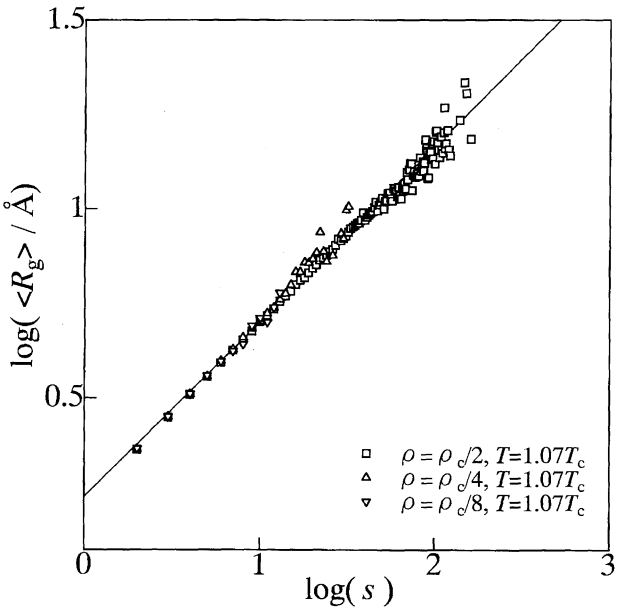

Fig. 5. Log–log plot of radius of gyration R_g of D-bond clusters against the cluster size s for SC water at various densities along the isotherm at $T = 1.07\ T_c$. The fractal dimension D evaluated from the slope was about 2.2.

between $2.2\rho_c$ and $3.4\rho_c$. The percolation density for hydrogen bonds is located in higher density region than that of the D-bonds. This may be caused by the fact that the necessary condition for the H-bond is rather more severe compared with that of the D-bond. Analyses of the H-bond clusters have been carried out for the fluid below the percolation density for the H-bond ($\rho \leqq 2.2\rho_c$).

In Fig. 6, the size distribution of the H-bond clusters is presented for the fluid at $\rho \leqq 2.2\rho_c$. The ordinate is such scaled that if the distribution follows Fisher's droplet model the plot gives a straight line. The plots show almost straight lines for all the densities below the percolation density for the H-bond. Thus, the size distribution of the H-bond clusters is again well described by the droplet model. Here, it is interesting to find the fact that the values of the parameters are the same as those adopted for the D-bond clusters, i.e., $\sigma = 0.5$ and $\tau = 2.1$.

In Table 2, averaged probabilities that particular topologies of the hydrogen bonds are found in the clusters of size $s = 3$ and 4 are listed for the fluid at various densities. It is clear that closely packed structures including looped bonds are seldom found. The averaged probabilities are much less than those for the D-bond clusters. This may arise from the fact that the hydrogen bond restricts not only the intermolecular distance but also orientation between the bonded molecules; it is difficult to form a loop structure by three or four hydrogen-bonded molecules. Thus, the H-bond clusters show much more bulky structures than those of the D-bond clusters. It is found, here, that the averaged probabilities have little density dependence, as in the case of the D-bond clusters. This will be discussed later again together with the density dependence of the other properties concerning the H-bond clusters.

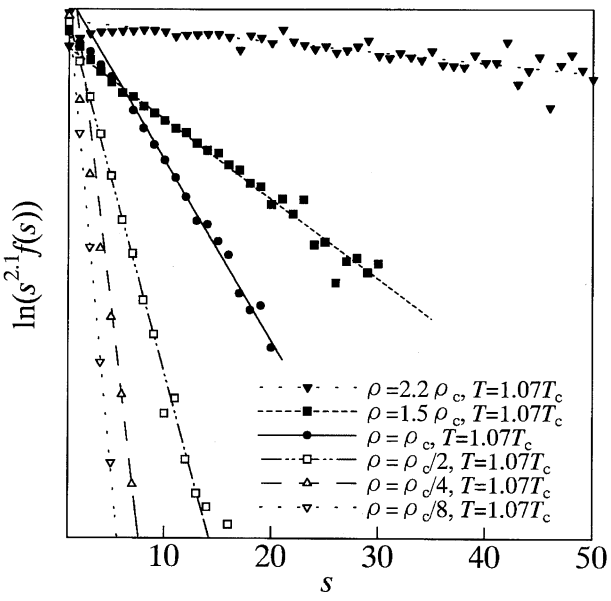

Fig. 6. Probability $f(s)$ that H-bond cluster is composed of s molecules for SC water at various densities along the isotherm at $T = 1.07\ T_c$. In the figure, $\log s^{\tau}f(s)$ is plotted against s where the values $\sigma = 0.5$ and $\tau = 2.1$ are adopted.

Table 2. Averaged Probability That Particular Topologies Are Found for the H-Bonds in the Clusters Whose Size is 3 and 4 for the Fluid at Various Densities

s=3	$2.2\rho_c$	$1.5\rho_c$	ρ_c	$\rho_c/2$	$\rho_c/4$	$\rho_c/8$
	0.00	0.00	0.01	0.01	0.01	0.01
	1.00	1.00	0.99	0.99	0.99	0.99
s=4	$2.2\rho_c$	$1.5\rho_c$	ρ_c	$\rho_c/2$	$\rho_c/4$	$\rho_c/8$
	0.00	0.00	0.00	0.00	0.00	0.00
	0.00	0.00	0.00	0.00	0.00	0.00
	0.01	0.01	0.01	0.01	0.01	0.02
	0.00	0.01	0.01	0.01	0.01	0.02
	0.81	0.81	0.82	0.82	0.82	0.81
	0.18	0.17	0.16	0.16	0.16	0.15

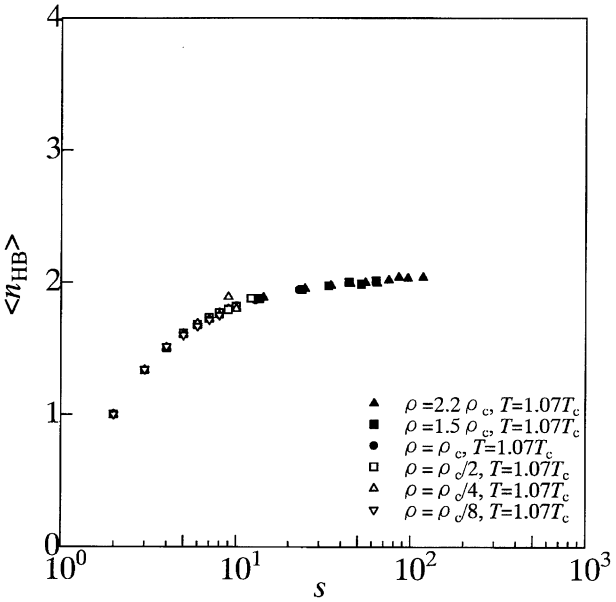

Fig. 7. Average number of H-bond per molecule $\langle n_{HB} \rangle$ as a function of cluster size s for SC water at various densities along the isotherm at $T = 1.07\ T_c$.

In Fig. 7, averaged number of the H-bonds per molecule $\langle n_{HB} \rangle$ is presented as a function of cluster size. As in the case of the D-bond cluster, $\langle n_{HB} \rangle$ increases quickly with increasing s for $s \leqq 10$. For larger clusters, $\langle n_{HB} \rangle$ increases relatively mildly and has a tendency to converge to a certain value. In Fig. 8, probability that a water molecule in a cluster has n_{HB} hydrogen bonds is presented for the fluid at various densities. The histogram is shown for the clusters in a few ranges of their size. For the cluster with $s = 9$, the ratio of molecules having one hydrogen bond is as large as about 40%. These molecules must be located at the surface.

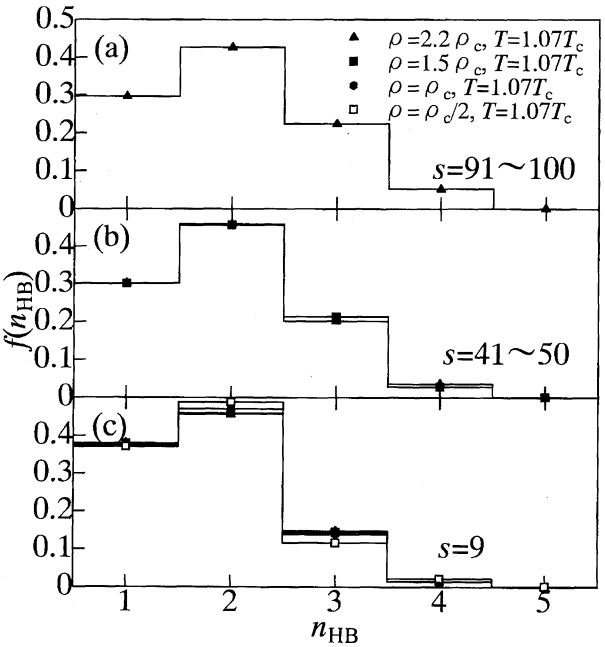

Fig. 8. Probability distribution of the number of H-bond per molecule n_{HB} for SC water at various densities for three classes of cluster size. (a) $s = 9$, (b) $41 \leqq s \leqq 50$, and (c) $91 \leqq s \leqq 100$.

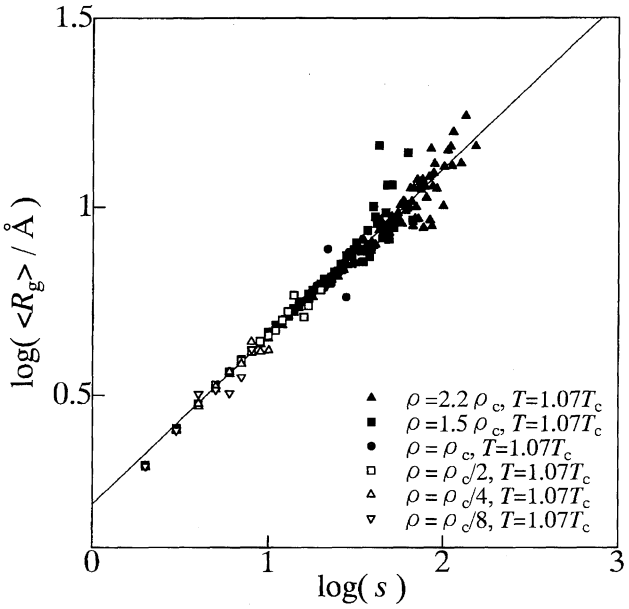

Fig. 9. Log–log plot of radius of gyration R_g of H-bond clusters against the cluster size s for SC water at various densities along the isotherm at $T = 1.07\ T_c$. The fractal dimension D evaluated from the slope was about 2.2.

Comparing the value with that for the D-bond clusters, 20%, it seems that the number of the surface molecules in the H-bond clusters is considerably greater than that for the D-bond clusters. Even in larger clusters, ($s > 40$) the molecules have higher occupancy at the perimeter than that in the D-bond clusters. This implies that the H-bond clusters have more bulky structures than those of the D-bond clusters. Further, the distribution is almost the same between the clusters with $s = 4$—50 and $s = 91$—100. As is the case of the large D-bond clusters, most water molecules are located at the surface of the cluster or at the perimeter of voids generated in the H-bond clusters. This causes the saturation of $\langle n_{HB} \rangle$ at the small value found for large clusters in Fig. 7.

In Fig. 9, a log–log plot of radius of gyration of the H-bond cluster is presented for the fluid at various densities as a function of cluster size. The plots approximately form a single straight line. The slope is about 2.2. This indicates that the H-bond clusters may be regarded as fractal, as in the case of the D-bond clusters. No difference in the dimension of the H-bond clusters from that of the D-bond clusters was found.

The static structure factor of $S_{HB}(k)$ "hydrogen bond density" is presented in Fig. 10 for the fluid at various densities. The hydrogen bond density was defined by considering a hydrogen bond as a particle. The location of the particle is at the middle between oxygen and hydrogen atoms which form the hydrogen bond. The static structure factor of the pseudo-particle density in k space gives $S_{HB}(k)$. Now, it is interesting to find that $S_{HB}(k)$ at $2.2\rho_c$ shows a relatively strong intensity in small k region compared with $S_{OO}(k)$. As stated above, the percolation density for the hydrogen bonds was found be-

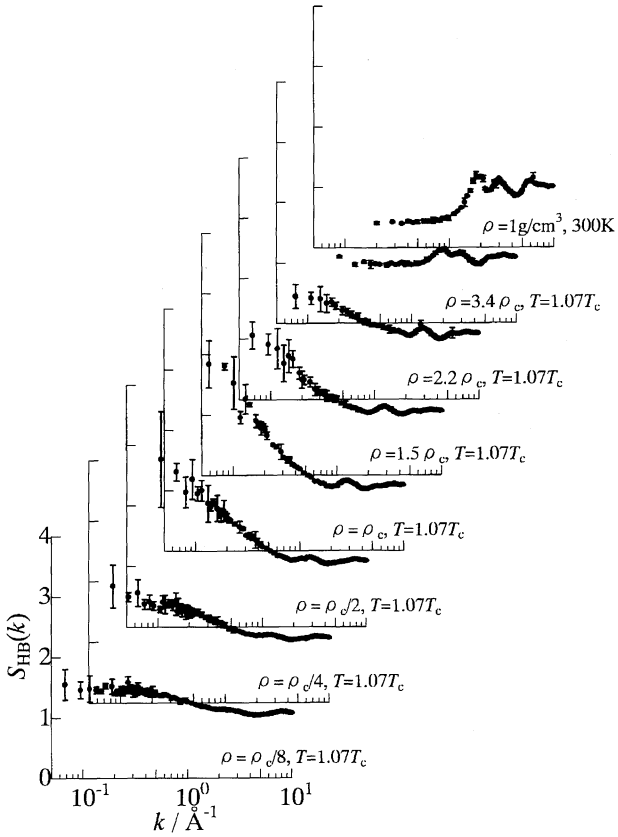

Fig. 10. Static structure factor of hydrogen bond density $S_{HB}(k)$ for SC water at various densities along the isotherm at $T = 1.07\ T_c$. For the definition of hydrogen bond density, see text. Error bars in the figure are the same as those in Fig. 1.

tween $3.4\rho_c$ and $2.2\rho_c$. Thus, it is likely that the percolation for the hydrogen bonds shows some critical phenomenon. However, even at $\rho < 2.2\rho_c$, the intensity in the small k region is still large, i.e. 1.5 ρ_c and ρ_c. This is reasonable because the critical density fluctuation of real molecules, i.e. $S_{OO}(k)$, gives a background intensity for $S_{HB}(k)$; a hydrogen bond is formed between real water molecules.

3. Dynamics of Clusters

In this section, the dynamics of clusters is discussed. Analyses have been carried out separately for D-bond and H-bond clusters.

D-Bond Clusters. Figure 11 presents snapshots of a D-bond cluster of size $s = 100$ along a trajectory for 2 ps. The figure clearly shows that, at $t = 0$, the cluster does not have a closely packed structure but a bulky structure, as discussed in the previous section. For $t < 0.5$ ps, while the cluster keeps the initial structure, the D-bond are locally broken. For longer time scale ($t > 0.5$ ps), the cluster collapses gradually due to spatial diffusion of the molecules.

In order to examine the above time-dependent properties quantitatively, we introduce an $N \times N$ bond matrix $\boldsymbol{A}$ where N is the total number of molecules in the system, i.e. $N = 1000$ in our case. Each matrix element represents bonding status between a given pair of molecules. For an instantaneous configuration of the fluid, the (i,j) element of the matrix a_{ij} is unity if i- and j-th molecules are bonded. Otherwise, $a_{ij} = 0$. The matrix may be rearranged such that a set of submatrices including non-zero elements along the diagonal line of $\boldsymbol{A}$ represent clusters and all the remaining matrix elements outside the submatrices are zero. An $s \times s$ submatrix corresponds to a cluster of size s. Since no bonds are found between different clusters, non-zero elements are all in the submatrices. The total number of the bonds in a cluster of size s is given by $(1/2) \sum_{i,j \in C_s} a_{ij}$ where C_s denotes a set of molecules belonging to the cluster of size s. For a cluster or a set of the molecules C_s defined at $t = 0$, the total number of bonds in the cluster changes along the trajectory due to bond breakage and restoration. This finally approaches zero for the infinitely large system. Thus, the time correlation function of the total number of bonds within the cluster can be defined as

$$B_{DB}(t) = \left\langle \sum_{i,j \in C_s} a_{ij}(t) \sum_{i,j \in C_s} a_{ij}(0) \right\rangle \Big/ \left\langle \left(\sum_{i,j \in C_s} a_{ij}(0) \right)^2 \right\rangle. \quad (2)$$

Here, C_s denotes the set of the molecules belonging to the cluster of size s defined at $t = 0$. Dynamical behavior of the correlation function reflects the relaxation processes of the cluster. The calculated correlation function $B_{DB}(t)$ is shown in Fig. 12 for the fluid at two densities, $\rho_c/2$ and $\rho_c/4$. The function is presented for a few selected size of the clusters. The correlation function for the fluid at lower densities is not shown due to insufficient statistics for large clusters. The figure clearly shows that $B_{DB}(t)$s have two-step relaxation processes. The faster one corresponds to the bond breakage occurring in the subpico second time scale. The slower one

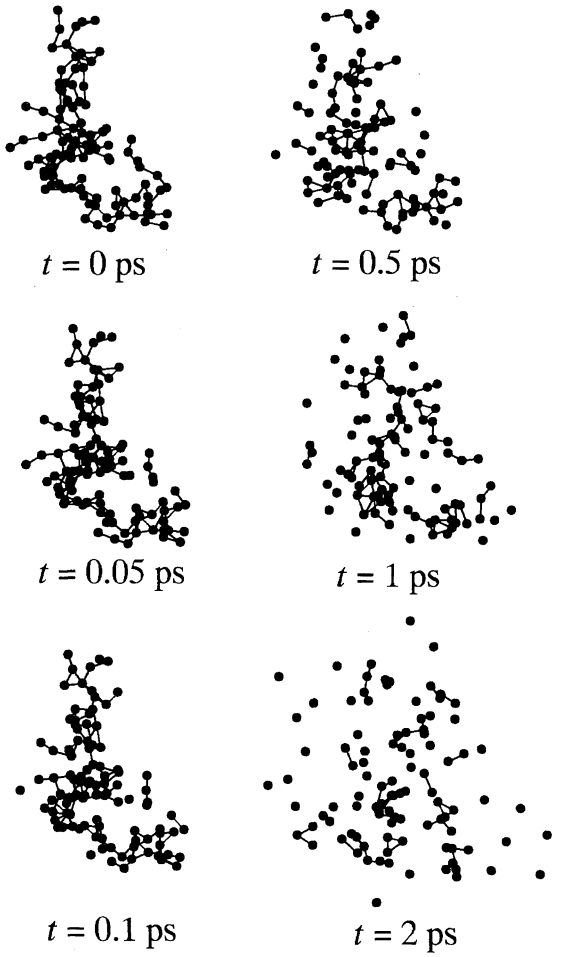

Fig. 11. Snap shots of a D-bond cluster of size $s = 100$ along a trajectory for 2 ps. Closed circles are oxygen atoms of water molecules in the cluster $t = 0$ ps. Solid lines represent intra-cluster D-bonds.

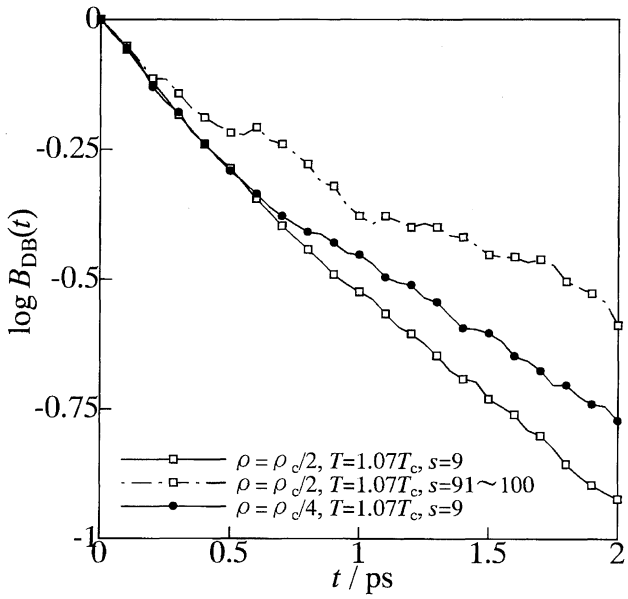

Fig. 12. Correlation function $B_{DB}(t)$ for SC water at two densities, $\rho = \rho_c/2$ and $\rho_c/4$. The figure is presented for selected sizes of the clusters, $s = 9$ and $s = 91$—100.

in a few pico seconds must be caused by the diffusion of the molecules. For large clusters, the latter relaxation is slower than that found in small clusters. It is also shown that $B_{DB}(t)$ at $\rho_c/2$ is approximately the same as that at $\rho_c/4$. In order to clarify density and cluster size dependence of the relaxation, the relaxation time of $B_{DB}(t)$ is plotted in Fig. 13 as a function of s for the fluid at various densities. The relaxation time τ_{DB} was evaluated by numerical integration of $B_{DB}(t)$. The relaxation time was corrected assuming an exponential decay of the function for large t. It is interesting to find that the clusters of the same size possess almost the same correlation time for the fluid at all densities except the lowest density $\rho_c/8$. The relaxation processes of the cluster are, thus, almost independent of the density. This might be related to the density-independent behavior of the structure of the clusters. With respect to the size dependent, the relaxation time becomes long with increasing s for all the densities below $\rho_c/2$. Thus, the larger cluster has the longer lifetime. Together with the cluster size distribution, this finding presents a molecular picture for the critical slowing down of space-time density–density correlations near the critical point.

The figure where the abscissa is logarithmically potted shows a roughly straight line. This implies that $\tau_{DB} \propto \log s$. High temperature clusters have fractallike bulky structure with a small number of bonds. This means that most of the component molecules may be considered as perimeter molecules. This gives a very slow increase of the lifetime of the clusters as a function of cluster size. This relation is in contrast to the case of the densely packed low temperature cluster where the relaxation time must increase more rapidly as a function of s than the logarithm.

In Fig. 14, the distribution of lifetimes of D-bond t_{DB} is presented for the fluid at various densities together with

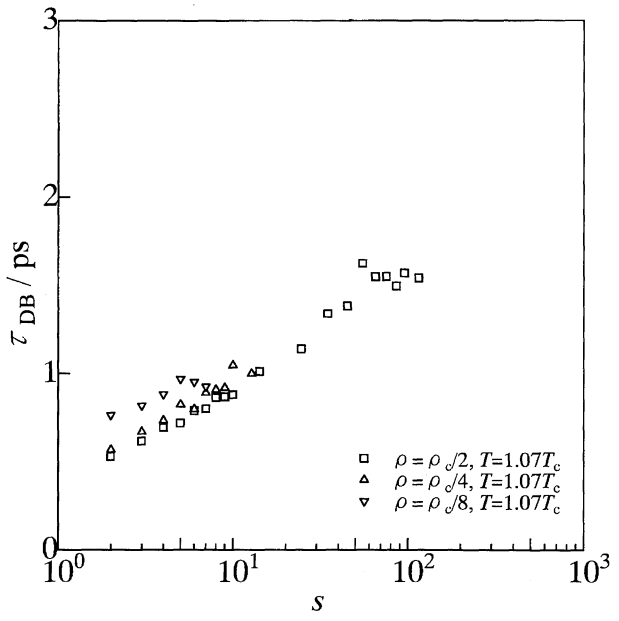

Fig. 13. Relaxation time of $B_{DB}(t)$ as a function of s for SC water at various densities along the isotherm at $T = 1.07\ T_c$.

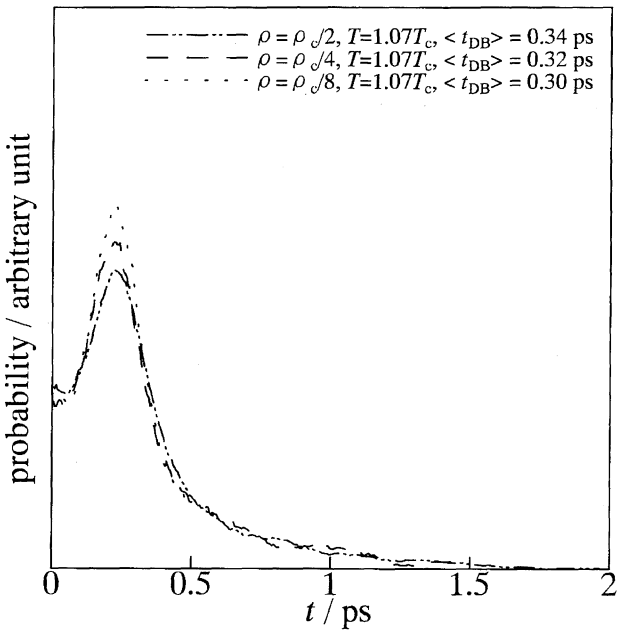

Fig. 14. Distribution of lifetime of the D-bond for SC water at various densities along the isotherm at $T = 1.07\ T_c$.

the averaged lifetime of the bond $\langle t_{DB} \rangle$. The lifetime was defined simply by the duration of bond such that a correction for the recombination of the bond was not made. The averged lifetime was in the range of 0.30—0.34 ps for these densities. Compared with the relaxation time of the total number of the D-bonds in the cluster τ_{DB}, the lifetime t_{DB} is about 3—5 times shorter than τ_{DB} for large clusters consisting of 10—100 molecules. Thus, the bond breakage occurs several times during the relaxation of the large cluster which requires structural rearrangement of the molecules in the clusters.

Hydrogen-Bonded Cluster. Time evolution of a hydrogen-bonded cluster of size $s = 104$ at $2.2\rho_c$ is presented in Fig. 15 for 2 ps. It is clearly shown that the bond breakage occurs very frequently compared with the D-bond cluster. The cluster kept its initial structure only for 0.1 ps. For $t \geqq 0.5$ ps, the cluster shows a diffuse structure, which comes from the diffusion of the molecules. These processes lead to the gradual decrease in the total number of the H-bonds in the cluster. In order to analyze the above processes quantitatively, we defined a bond matrix $\boldsymbol{A}$ again for the hydrogen bond in the same way as in the case of the D-bond clusters. The matrix element of $\boldsymbol{A}$, a_{ij}, is unity for hydrogen-bonded pair. Otherwise, $a_{ij} = 0$. Using the matrix, the autocorrelation function of the bond number can be defined in the same way as shown in Eq. 2. The calculated result is presented in Fig. 16 for the fluid at two densities, $2.2\rho_c$ and $1.5\rho_c$. The function is shown for selected cluster sizes, $s = 9$ and 91—100. The calculated time correlation functions show two-step relaxation processes as found in the case of the D-bond clusters. The faster one is found within about 0.1 ps and the slower one is in the pico second region. The faster decay is caused by the very frequent bond breakage in the cluster shown in Fig. 15. In order to examine this short-time decay, distribution of lifetimes of the hydrogen bond was plotted

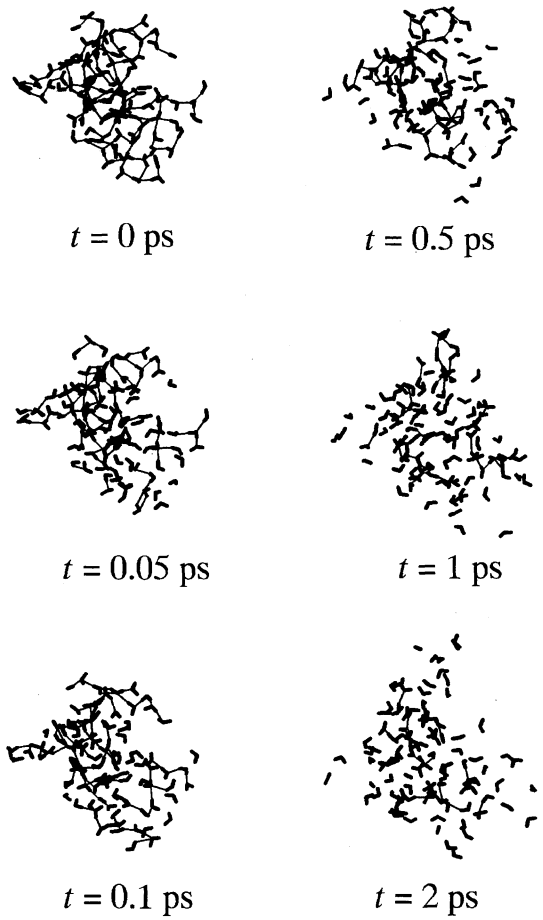

Fig. 15. Snap shots of a hydrogen-bonded cluster of size $s = 104$ at $2.2\rho_c$ along a trajectory for 2 ps. Thick lines are water molecules. Thin lines represent intra-cluster H-bonds.

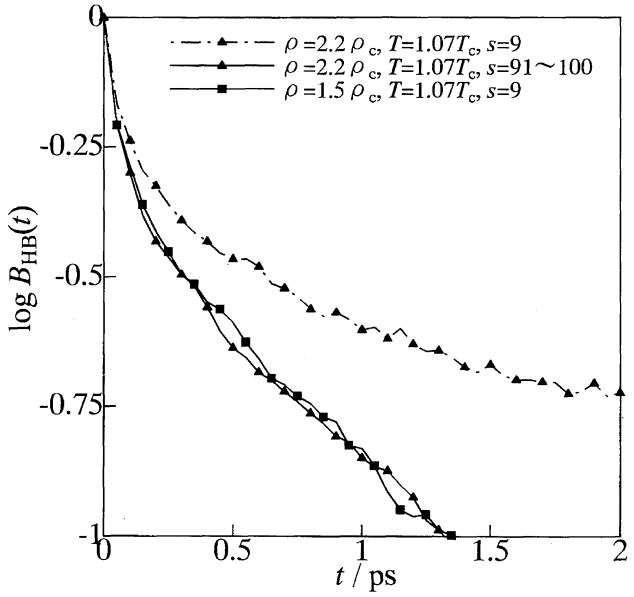

Fig. 16. Correlation function $B_{HB}(t)$ for SC water at two densities, $\rho = 2.2\rho_c$ and $1.5\rho_c$. The figure is presented for selected sizes of the clusters, $s = 9$ and $s = 91$—100.

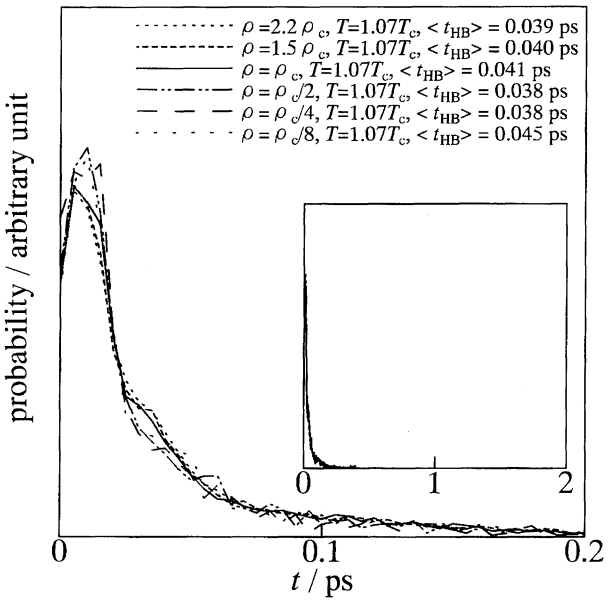

Fig. 17. Distribution of lifetime of the H-bond for SC water at various densities along the isotherm at $T = 1.07\ T_c$.

in Fig. 17 for the fluid at various densities. It is found that the distribution is almost the same along the isotherm at 1.07 T_c. The average lifetime is about 0.04 ps. This demonstrates that the breakage of a hydrogen bond occurs within a very short time. The time scale is in correspondence to that of the faster relaxation found in $B_{HB}(t)$.

The slower relaxation comes from the diffusion of the molecules, which leads the cluster to the collapse. The large difference in time scale between the bond breakage and the molecular diffusion makes the two-step relaxation clear compared with the case of the D-bond clusters. In Fig. 18, the relaxation time of $B_{HB}(t)$ is presented as a function of s for the fluid at various densities. The relaxation time was evaluated

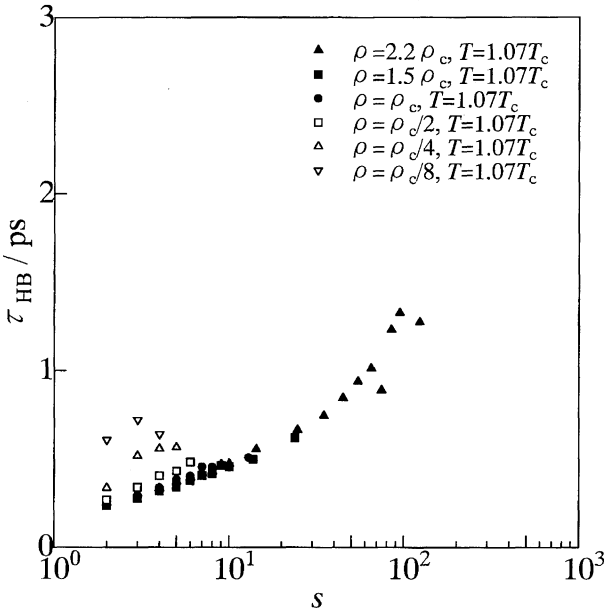

Fig. 18. Relaxation time of $B_{HB}(t)$ as a function of s for SC water at various densities along the isotherm at $T = 1.07\ T_c$.

by the same method as described in the previous subsection. As clearly shown in the figure, the relaxation time of the H-bond clusters is short compared with that of the D-bond clusters. For the clusters consisting of about 100 molecules, the relaxation time is about 1.3 ps, which is about 30 times as long as the average lifetime of the H-bond. This indicates that the cluster gradually disperses by the diffusion of the molecules, repeating the bond creation and annihilation forty or fifty tens times. The figure also shows that the relaxation time becomes long with increasing cluster size. As reported above, a slow relaxation of the large D-bond clusters leads to the slowing down of the dynamic density–density correlations near the critical point. Similarly, the slow relaxation of the large H-bond clusters may cause the slowing down of the space-time correlations of the properly defined hydrogen bond density. For relatively large clusters up to about $s = 30$, logarithmically scaled relaxation time, $\tau \propto \log s$, is again observed. For larger clusters, however, systematic deviation from the logarithmic dependence on s is noticeable. This suggests that there is a different relaxation process in the large H-bond clusters from that found in the D-bond clusters.

4. Conclusion

A series of MD calculations of SC water have been performed. The calculated $S_{OO}(k)$ in small k region showed strong intensity for the fluid near the critical densities, reflecting long-ranged density–density correlation. Analysis of the density fluctuation has been carried out using a concept of "cluster," which was defined by a set of water molecules linked with each other by "bonds." In this paper, two kinds of bonds were investigated. One is a bond defined simply by oxygen–oxygen distance (D-bond). The other is a hydrogen bond (H-bond). As found in the LJ fluids, percolation transition of the D-bond was found for the present SC water near the critical point. Below this density, the system is separated into various sizes of the clusters. It was also found that the distribution of the cluster size may be well described by Fisher's droplet model. The clusters have bulky structures. The analysis of R_g as a function of cluster size showed that the high temperature clusters have fractal character. These are in contrast to the case of the low temperature clusters. It was also found that various properties of the clusters along the isotherm are almost independent of the density. Thus, SC water below the critical density may be regarded as an ensemble of the density-independent clusters. Just the size distribution of the clusters changes as a function of the fluid density. It was demonstrated, too, that the larger cluster has the longer relaxation time. This may present a molecular picture of the critical slowing down of intermediate scattering function of SC water.

The hydrogen-bonded clusters presented another view of SC water. It was found that the percolation transition for the hydrogen bonds occurs well above critical density. This arises from the fact that the definition of the hydrogen bond is severer than that of the D-bond. The size distribution of the hydrogen-bonded clusters is again well described by Fisher's droplet model. The bulky nature of the H-bond clusters, which have fractal character, was also observed. No difference in the fractal dimension of the hydrogen-bonded clusters from that of the D-bond clusters was found in the present calculations. With respect to the dynamical behavior, for larger clusters, cluster size dependence of the relaxation time is different between D- and H-bond clusters. This suggests that there is a different relaxation process in the large H-bond clusters from that found in the D-bond clusters. The lifetime of the clusters becomes longer with increasing cluster size. This may lead to the slowing down of the space-time correlation of properly defined "hydrogen bond density" or some relevant physical properties. The lifetime of the H-bond clusters was shorter than that of the D-bond clusters.

The authors thank the computer centers of the Institute for Molecular Science, Tokyo Institute of Technology, and Japan Atomic Energy Research Institute for the use of supercomputers. The work was supported in part by Grants-in-Aid for Scientific Research Nos. 09740419, 09440197, and 09216204 from the Ministry of Education, Science, Sports and Culture. N. Y. has been supported by the Japan Society for the Promotion of Science for Japanese Junior Scientists.

References

1) E. Kiran and J. M. H. Levelt Sengers, "Supercritical Fluid: Fundamentals for Application," Kluwer, Dordrecht (1994).

2) T. J. Bruno and J. F. Ely, "Supercritical Fluid Technology: Reviews in Modern Theory and Application," Chemical Rubber, Boca Raton, FL (1991).

3) E. V. Bright and M. E. P. McNally, "Supercritical Fluid Technology," ACS Symposium Series Vol. 488, American Chemical Society, Washington D.C. (1992).

4) E. Kiran and J. F. Brennecke, "Supercritical Fluid Engineering Science," ACS Symposium Series Vol. 514, American Chemical Society, Washington D.C. (1993).

5) M. D. Luque de Castro, M. Valcarcel, and M. T. Tena, "Analytical Supercritical Fluid Extraction," Springer-Verlag, Berlin (1994).

6) V. Krukonis, G. Bruuner, and M. Perrut, "Proc. 3rd Int. Symp. Supercritical Fluids," Strasburg (1994), No. 1, p. 1.

7) C. A. Eckert, B. L. Knutson, and P. G. Debenedetti, *Nature*, **383**, 313 (1996).

8) C. A. Eckert, D. H. Ziger, K. P. Johnston, and S. J. Kim, *J. Phys. Chem.*, **90**, 2738 (1986).

9) J. V. Sengers and J. M. H. Levelt Sengers, *Ann. Rev. Phys. Chem.*, **37**, 189 (1986).

10) "NIST Standard Reference Database," **10**, (1996).

11) D. Eisenberg and W. Kauzmann, "The Structure and Properties of Water," Clarendon, Oxford (1969).

12) S. T. Cui and J. G. Harris, *J. Phys. Chem.*, **99**, 2900 (1995).

13) N. Yoshii and S. Okazaki, *J. Chem. Phys.*, **107**, 2020 (1997).

14) a) R. Ishii, S. Okazaki, I. Okada, M. Furusaka, N. Watanabe, M. Misawa, and T. Fukunaga, *J. Chem. Phys.*, **105**, 7011 (1996); b) R. Ishii, S. Okazaki, I. Okada, M. Furusaka, N. Watanabe, M. Misawa, and T. Fukunaga, *Mol. Phys.*, **95**, 43 (1998).

15) a) H. Guittinger and D. S. Cannell, *Phys. Rev.*, **A22**, 285 (1980); b) J. D. Londono, V. M. Shah, G. D. Wignall, H. D. Cochran, and P. R. Bienkowski, *J. Chem. Phys.*, **99**, 466 (1993); c) T. Morita, H. Miyagi, Y. Shimokawa, H. Matsuo, and K. Nishikawa, *Jpn. J.*

Appl. Phys., **37**, L768 (1998).

16) H. E. Stanley, "Introduction to Phase Transition and Critical Phenomena," Clarendon, Oxford (1971).

17) a) P. Postrino, R. H. Tromp, M. A. Ricci, A. K. Soper, and G. W. Neilson, *Nature*, **366**, 668 (1993); b) R. H. Tromp, P. Postrino, G. W. Neilson, M. A. Ricci, and A. K. Soper, *J. Chem. Phys.*, **101**, 6210 (1994); c) A. K. Soper, F. Bruni, and M. A. Ricci, *J. Chem. Phys.*, **106**, 247 (1997); d) A. Botti, F. Bruni, M. A. Ricci, and A. K. Soper, *J. Chem. Phys.*, **109**, 3180 (1998).

18) a) K. Yamanaka, T. Yamaguchi, and H. Wakita, **101**, 9830 (1994); b) M. M. Hoffmann and M. S. Conradi, *J. Am. Chem. Soc.*, **119**, 3811 (1997); c) N. Matubayasi, C. Wakai, and M. Nakahara, *Phys. Rev. Lett.*, **78**, 2573 (1997); d) N. Matubayasi, C. Wakai, and M. Nakahara, *J. Chem. Phys.*, **107**, 9133 (1997).

19) a) Y. Guissani and B. Guillot, *J. Chem. Phys.*, **98**, 8221 (1993); b) A. Famular, R. Specchio, and M. Raimondi, *J. Chem. Phys.*, **108**, 3296 (1998); c) P. Jedlovszky, J. P. Brodholt, F. Bruni, M. A. Ricci, A. K. Soper, and R. Vallauri, *J. Chem. Phys.*, **108**, 8528 (1998); d) A. G. Kalinichev and J. D. Bass, *J. Phys. Chem.*, **A101**, 9720 (1997); e) R. D. Mountain, *J. Chem. Phys.*, **90**, 1866 (1989); f) R. D. Mountain, *J. Chem. Phys.*, **103**, 3084 (1995); g) R. D. Mountain, *NIST Technical Rep.*, **1997**, 6028; h) R. D. Mountain, *Rev. High Pressure Sci. Technol.*, **7**, 1106 (1998); i) L. X. Dang, *J. Phys. Chem.*, **B102**, 620 (1998); j) G. Löffler, H. Schreiber, and O. Steinhauser, *Ber. Bunsenges. Phys. Chen.*, **98**, 1575 (1994); k) P. T. Cummings, H. D. Cochran, J. M. Simonson, R. E. Mesmer, and S. Karaborni, *J. Chem. Phys.*, **94**, 5606 (1991); l) E. S. Fois, M. Sprik, and M. Parrinello, *Chem. Phys. Lett.*, **223**, 411 (1994); m) T. I. Mizan, P. E. Savage, and R. M. Ziff, *J. Phys. Chem.*, **98**, 13067 (1994); n) T. I. Mizan, P. E. Savage, and R. M. Ziff, *J. Phys. Chem.*, **100**, 403 (1996); o) A. A. Chialvo and P. T. Cummings, *J. Chem. Phys.*, **101**, 4466 (1994); p) A. A. Chialvo and P. T. Cummings, *J. Phys. Chem.*, **100**, 1309 (1996); q) M.-C. Bellissent-Funel, T. Tassaing, H. Zhao, D. Beysens, B. Guillot, and Y. Guissani, *J. Chem. Phys.*, **107**, 2942 (1997); r) A. A. Chialvo and P. T. Cummings, *J. Chem. Phys.*, **105**, 8274 (1996); s) I. M. Svishchev, P. G. Kusalik, J. Wang, and R. J. Boyd, *J. Chem. Phys.*, **105**, 4742 (1996).

20) M. E. Fisher, *Physics*, **3**, 255 (1967).

21) M. E. Fisher, *Rep. Progt. Phys.*, **30**, 6150 (1967).

22) C. Domb and M. S. Green, "Phase Transition and Critical Phenomena," Academic Press, London (1974), Vol. 3.

23) a) D. Stauffer, "Introduction to Percolation Theory," Taylor & Francis, London (1985); b) D. Stauffer, *Phys. Reports*, **54**, 1 (1979).

24) N. Yoshii and S. Okazaki, *Fluid Phase Equil.*, **144**, 225 (1998).

25) W. Gebhardt and U. Krey, "Phase Transition and Critical Phenomena," Frider, Vieweg & Sohn, Braunschweig (1980).

26) J. J. Binnery, N. J. Dowrick, A. J. Fisher, and M. E. J. Newman, "The Theory of Critical Phenomena," Clarendon, Oxford (1992).

27) J. M. Yeomans, "Statistical Mechanics of Phase Transitions," Clarendon, Oxford (1992).

28) L. X. Dang, *J. Chem. Phys.*, **97**, 2659 (1992).

29) N. Yoshii, H. Yoshie, S. Miura, and S. Okazaki, *J. Chem. Phys.*, **109**, 4873 (1998).

30) N. Yoshii, H. Yoshie, S. Miura, and S. Okazaki, *Rev. High Pressure Sci. Technol.*, **7**, 1115 (1998).

31) A. G. Kalinichev and J. D. Bass, *Chem. Phys. Lett.*, **231**, 301 (1994).

32) B. L. Holian and D. E. Grady, *Phys. Rev. Lett.*, **60**, 1355 (1988).

33) D. Chandler, "Introduction to Modern Statistical Mechanics," Oxford, New York (1987).

34) J. Rudnick and G. Gaspari, *Science*, **237**, 384 (1987).

35) D. M. Heyes and J. R. Melrose, *Mol. Phys.*, **66**, 1057 (1989).